

Mechanism for self-formation of periodic structures on a plastic polymer surface using a nanoseconds and femtosecond laser pulse

Behzad Mansouri*, P.Parvin

Department of Physics, Amirkabir University of Technology, Hafez Ave, Tehran, Iran P.O. Box: 15875-4413

*Corresponding author. behzad.mansouri@hotmail.com

The high UV laser dose at 193 nm induces grooves on poly allyl diglycol carbonate PADC (CR39) at normal irradiation. The spatial period exhibits to be nearly invariant for azimuth and polar angles indicating a loose dependence on the incident angles but the LIPSS (Laser-induced periodic surface structures) are always parallel to the P polarization component of the incident beam. The most common approach to explain LIPSS formation is related to the Sipe theory which does not account for all the observed phenomena especially LIPSS with periodicity larger than the laser wavelength. In fact the LIPSS is a multi parameter mechanism based on surface rippling, acoustic modulation and laser ablation and etc. In experiment with CR-39 polymer, laser irradiation produce a very tiny melting layer of mixture of monomer due to depolymerization on the surface and it seems capillary wave is responsible for grooves (fringe pattern) formation.

Keywords: LIPSS, Groove, Plasmon wave, capillary wave

I. INTRODUCTION

Laser-induced periodic surface structures (LIPSS) have been studied since the 1960s [1] appear on dielectric, semiconductor, polymer and metal surfaces exposed to single or multiple short and ultra short laser pulses [1,2]. The most common LIPSS, that refer to as ripples, consist of wavy surfaces which can be produced on metals [2], semiconductors [3], dielectrics [4] and polymers [5]. When created with linearly polarized laser radiation at normal incidence, these ripples show a periodicity close to the laser wavelength, Ripples having these properties are usually attributed to as low spatial frequency LIPSS (LSFL). Furthermore a new kind of ripples has been recently observed. Applying picoseconds or femtosecond laser pulses, the ripples with a periodicity significantly smaller than the laser wavelength, referred to as high spatial frequency LIPSS (HSFL). LIPSS with periodicities larger than the laser wavelength have also been observed similar to those referred in [1]. Experiment, irradiation of CR39 sample with excimer nanosecond laser. These LIPSS, usually looks like as “grooves” [6]. Although, the exact physics of their formation remains unexplained we investigate the formation mechanism from different points of view in this paper.

II. ELECTROMAGNETIC APPROACH

It is generally accepted that LSFL formation is driven by the interaction of electromagnetic waves with the rough surface of materials [3]. Considering surface roughness that may shift the dispersion curve leads to coupling between the surface plasmon wave and the incident laser pulse.

However above mechanism can be dominant after several few shots to induce some roughness on our initial sample, the experimental observation demonstrated that grooves as shown in Fig.1 can take place even after first shots.

The LIPSS mechanism for metals has been also explained with excitation of the surface plasmon polariton (SPP) [7, 8]. The femtosecond pulse plasma lengths scale is very short and we consider surface plasma. SPPs are electromagnetic excitations propagating at the interface between a dielectric and an electrically conductive material. Indeed, the ripple formation links to SPP in the case of semiconductor material like silicon using femtosecond pulses. Although, the generation of surface plasmon is due to the presence of free electron at the interface of two materials that implies one of material should be a metal, it is proposed that under ultra-short laser exposure the optical properties of dielectrics change in to the metallic. Regarding this consideration SPP excitation can be achieved. The parametric process of photon→photon+plasmon is referred to as stimulated Raman scattering where an incident photon decays into Plasmon and a scattered photon at lower frequency. Sakabe et al [8] showed that ripples periodicity is shorter than the laser wavelength under femtosecond irradiation. (The dispersion relation of surface plasmon showed that the periodicity is ranging 0.85-0.5 of laser wavelength. While SPPs can explain a periodicity Λ of LSFLs smaller than the laser wavelength ($\Lambda \leq \lambda$), it is unclear why Λ depends on the fluence and decreases with the number of pulses applied. Only a few studies on the formation of LIPSSs with a periodicity larger than the laser wavelength ($\Lambda > \lambda$) are reported in literature. In our setup the spatial period Λ exhibits to be nearly invariant for azimuth ϕ and polar θ

angles indicating a loose dependence on the incident angles. However, the created lines are always parallel with the P polarization component of the incident beam. For nanosecond pulse the front phase of a laser pulse heats sample, which turns into plasma. The plasma is heated by the tail of the pulse due to IB absorption (Inverse Bremsstrahlung) which expands at sonic speed. Consequently, the major part of the pulse makes more dense bulk plasma. Direct coupling laser pulse with plasma wave occurs when plasma frequency increase with increasing laser fluence as long as to match with laser frequency. Let assume grooves formation in our experiment on CR39 sample occurs due to plasma wave, increasing the fluence will lead to increase plasma density, $n \propto F$ and as well as plasma frequency $\omega^2 = n(4\pi e^2) / m$, that makes decrease in wavelength and periodicity. Even in femtosecond case, surface electron density, n' proportioned with n/v , v is plasma velocity that proportionate with \sqrt{T} , so $n' \propto n/v \propto F^{1/2}$. As one can see both case leads to inverse relation between periodicity and laser fluence. This model does not completely match with the observation that illustrated in Fig 2 [9].

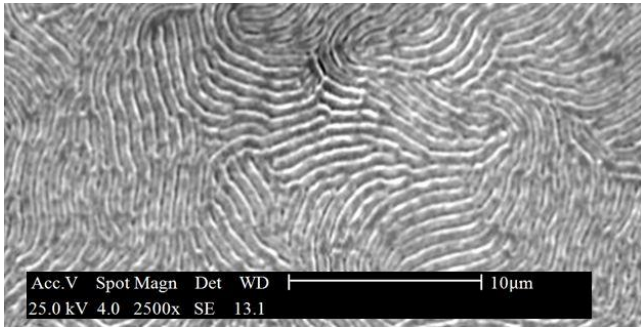


Figure 1: Laser-induced periodic surface structures on CR39 implied fringe pattern distribution. The fringe width or periodicity increase with increasing laser fluence within ranging 0.7- 0.8 μm [9].

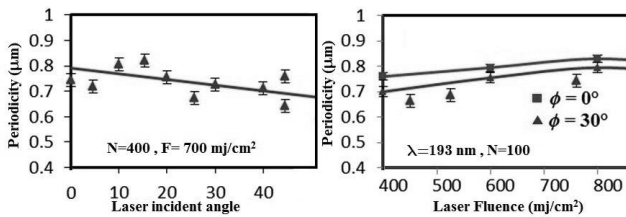


Figure 2: Grooves periodicity versus incident fluence at $\phi=0^\circ$ (rectangles) and $\phi=30^\circ$ (triangles) incident angles and versus incident fluence [9].

III. LASER INDUCED CAPILLARY WAVE

The exact theoretical description of all physical process is so extensive and complicated. In this paper we present

concise analytical models. We consider capillary wave formation due to presence of surface tension in the molten layer on the surface due to depolymerization of polymer as a mechanism for self-formation of periodic fringe patterns at normal incidence.

ArF laser (LPX 220i, Lambda Physik) was employed with 15 ns duration and 1 Hz repetition rate to be spatially distributed over $\sim 0.9\text{cm} \times 2.5\text{cm}$ beam cross-section (CR39 sheets was cut in to $1.5\text{mm} \times 10\text{mm} \times 10\text{mm}$), is focused on samples through a cylindrical MgF_2 lens ($f = 20\text{ cm}$) [9]. The laser profile is uniform in X direction and hat-top in Y direction which produces temperature gradient within the thickness of sample obviously but no temperature gradient across the thickness, so with this consideration, surface tension is constant and we can ignore Marangoni flow effect. Samples have been irradiated with various fluences, with multiple shot numbers and create melting layer on surface which become cool and solid before the next pulse comes (according to our calculation the order of magnitude of melting life time is about 1.6 μs and time duration between pulse is 1s). For estimation spatial period length we start from dispersion relation for capillary wave as below formula [10, 11]:

$$\omega = \sqrt{k\left(g + \frac{\alpha k^2}{\rho}\right) \tanh(kh)} \quad (1)$$

With rearranging based on wavelength we have:

$$\lambda = \sqrt{\frac{1}{2} g h \tau^2 + \frac{\sqrt{h} \tau \sqrt{16\pi^2 \alpha + g^2 h \tau^2} \rho}{2\sqrt{\rho}}} \quad (2)$$

For small wavelength only surface tension is dominant and we ignore gravity effect so we reduce equation into:

$$\lambda = \sqrt[4]{\frac{\alpha h}{\rho}} (2\pi\tau)^{1/2}. \quad (3)$$

Where λ is the wavelength of the capillary wave, α , h , ρ and τ are the surface tension coefficient, melt depth, mass density and period of wave respectively. Note that wave cannot exist more than life time of melting layer, so we can replace τ with τ_{melt} .

CR-39 is a thermosetting plastic and cannot be melted in general. But when laser pulses interact with sample, a lot of processes due to photothermal, photochemical occurs and consequently led to depolymerization of polymer into mixtures of monomers just on the surface of sample and finally change the optical, thermophysical properties. However the exact nature of the decomposed product was not analyzed yet but the product of laser-induced decomposition can be existed in liquid. With considering thermogravimetric analysis of heat treated CR-39 polymer [12], melting is observed as small peak in the DTG plot of derivative weight against temperature.

Depending on type of laser pulse (short or ultra short) analyzing and modeling of laser ablation process and melting dynamic may be changed. In the case of femtosecond, because of shockwave presence, the mechanism would not be simple. The energy transport in ultrashort laser heating is two stages process. At first the absorption of the laser energy through photon-electron interactions within the ultrashort pulse duration and electrons reestablish the Fermi distribution in just a few femtoseconds. The second stage is the energy distribution to the lattice through electron-phonon interactions, on the order of tens of picoseconds. Two-temperature model is necessary in order to describe the exact thermal process.

In the nanosecond case, the process can be modeled by heat conduction, melting and plasma formation. For estimation of melting thickness; first we consider temperature profile as below:

$$T_{melting} - T_{initial} = \frac{F}{\rho C \delta_p}, \quad (4)$$

T_{melt} is the working point temperature at which the sample can easily be formed with viscosity less than 10^3 Pa.s. δ is optical penetration depth and F is absorbed laser energy fluence given by Beer –Lambert absorption law in term of incident fluence or fluence threshold and ablation depth:

$$F = AF_i \exp\left(-\frac{z}{\delta_p}\right) = AF_{th} \exp\left(-\frac{z-h_a}{\delta_p}\right), \quad (5)$$

we get a formula for initial melting thickness as below:

$$h_M = \delta_p \ln\left(\frac{AF_{th}}{(T_M - T_i) \rho C \delta_p}\right), \quad (6)$$

For estimation of the surface absorptivity (A), we should note that however CR-39 is completely opaque in the UV range and in fact the reflectivity can be derived by the Fresnel equation which is about 4% in this case, but when sample is radiated with high fluence of laser pulses, reflectivity increases as the plasma density increases. So with presence of the dense plasma, most of incident laser energy is reflected back from the surface (induced skin effect). Infact most of energy is used by the expanding plasma. We observed that when the incident laser fluence is higher than threshold (applied fluence $700 \text{mj/cm}^2 > F_{th} \approx 225 \text{mj/cm}^2$), plasma with a critical density can be formed and a large portion of the energy is reflected from the sample.

For estimation of the average melt time, we need to see variation of temperature with time and place. According to our initial and boundary conditions, the solution of diffusion equation would be in terms of erfc as below:

$$\frac{\partial T}{\partial t} = D \frac{\partial^2 T}{\partial z^2}, \quad (7)$$

$$T(z, 0) = T_i + \frac{AF_i}{\rho C \delta_p} \exp\left(-\frac{z}{\delta_p}\right), \quad (8)$$

Non-dimensionalized equation provides better insight into relative size of terms, so we have:

$$T' = \frac{\rho C \delta_p}{AF_i} (T - T_{initial}), \quad (9)$$

$$z' = \frac{z}{\delta_p}, t' = \frac{D}{\delta_p^2} t, \quad (10)$$

Finally we obtain a analytical solution for temperature distribution as below:

$$T'(z', t') = \frac{\int_0^\infty e^{-a} \left[e^{-\frac{(z'+a)^2}{4t'}} + e^{-\frac{(z'-a)^2}{4t'}} \right] da}{(4\pi t')^{1/2}}, \quad (11)$$

$$T'(z', t') = \frac{e^{t'-z'}}{2} \left(\text{Erfc}\left[-\frac{-2t'+z'}{2\sqrt{t'}}\right] + e^{2z'} \text{Erfc}\left[\frac{2t'+z'}{2\sqrt{t'}}\right] \right). \quad (12)$$

Now we can estimate both initial melt depth and average melt time. The average melt depth varies between 0.2 and $0.4 \mu\text{m}$ and the average of melt lifetime varies between $0.8 \mu\text{s}$ and $1.6 \mu\text{s}$. We used the thermophysical properties of decomposed products as mixture of monomers on average in our calculation [13,14,15,16].

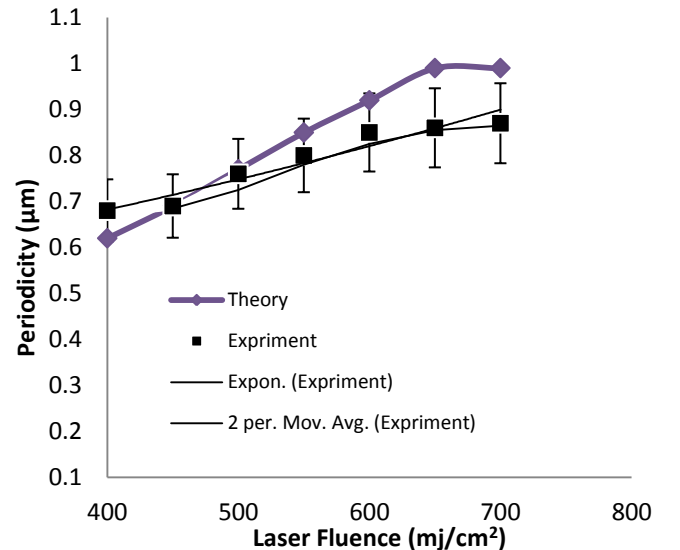


Figure 3: Comparison of the rather agreement between theory and experiment for periodicity versus incident laser fluence at normal incidence.

In summary, as shown in Fig.3, the increasing of periodicity with increasing laser fluence is consistent with capillary wave-driven formation. With increasing laser

fluence lead to more deposited energy in the sample and melting more and make increase in liquid layer depth and consequently life time. Dispersion formula (3) shows us that longer life time and liquid depth we have longer capillary wavelength and obviously longer periodicity. From the discussion above, it is concluded that several models have been proposed in articles. However, none of the proposed models can account for all the observed LIPSS and their various properties. In fact the LIPSS is a multi parameter mechanism based on surface rippling, acoustic modulation and laser ablation and etc. A complete theory should also explain the variation of periodicity of LSFL and possible change of orientation from HSFL to LSFL, as observed in many experiments. .

[1] Birnbaum, Semiconductor surface damage produced by ruby lasers, *J.Appl.Phys.*36 (1965)3688.
 [2] Y.Jee, Michael F.Becker, and Rodger M.Walser. Laser-induced damage on single-crystal metal surfaces. *Journal of the Optical Society of America B*, 5:648–659, 1988.
 [3] D.C.Emmony, R.P.Howson, and L.J.Willis. Laser mirror damage in germanium at 10.6 μm . *Applied Physics Letters*, 23:598–600, 1973.
 [4] P.Temple and M.Soileau. Polarization charge model for laser-induced ripple patterns in dielectric materials. *IEEE Journal of Quantum Electronics*, 17:2067–2072, 1981.
 [5] S.Baudach, J.Bonse, and W.Kautek. Ablation experiments on polyimide with femtosecond laser pulses. *Applied Physics A: Materials Science & Processing*, 69:S395–S398, 1999.
 [6] J.Bonse, M.Munz, and H.Sturm. Structure formation on the surface of indium phosphide irradiated by femtosecond laser pulses. *Journal of Applied Physics*, 97:013538–1–9, 2005.
 [7] J.E.Sipe, J.F.Young, J.S.Preston, H.M.vanDriel, Laser-induced periodic surface structure. i.theory, *Phys.Rev.B*27 (1983)1141–1154.
 [8] S.Sakabe. *Physical Review B* 79, p. 033409 (2009).
 [9] Angular dependence of ArF laser induced self-aligning microstructures on CR39 Optical Materials *Express* Vol. 5, Issue 7, pp. 1543-1549 (2015)
 [10] L.D. Landau & E.M. Lifshitz *Fluid Mechanics* (Volume 6 of a Course of Theoretical Physics)
 [11] *Fluid mechanics* / Pijush K. Kundu, Ira M. Cohen, David R. Dowling. – 5th ed
 [12] Thermogravimetric analysis of heat treated CR-39 polymer Renu Gupta*, V. Kumar, P.K. Goyal and Shyam Kumar *J. Chem. Pharm. Res.*, 2010, 2(4):629-634

[13] Parviz Parvin, Babak Jaleh, N. Sheikh, N. Amiri, “Surface Effect of KrF Laser Exposure on ECE of Alpha Particle Tracks in Polycarbonate Polymer”, *Radiation Measurements*, Vol. 40, No.2-6, PP. 775 – 779, (2005).
 [14] *Polymeric Materials Encyclopedia*, Twelve Volume Set by Joseph C. Salamone
 [15] Lytle, J.D. 1995. *Handbook of Optics*, Vol. 2, 2nd ed., p. 34.1. McGraw-Hill, New York; and Wolpert,
 [16] James E Mark-Physical properties of polymers handbook-Springer (2007)